

Excitation of propagating spin waves with global uniform microwave fields

Y. Au, T. Davison, E. Ahmad, P. S. Keatley, R. J. Hicken et al.

Citation: *Appl. Phys. Lett.* **98**, 122506 (2011); doi: 10.1063/1.3571444

View online: <http://dx.doi.org/10.1063/1.3571444>

View Table of Contents: <http://apl.aip.org/resource/1/APPLAB/v98/i12>

Published by the [American Institute of Physics](#).

Related Articles

Reciprocal Damon-Eshbach-type spin wave excitation in a magnonic crystal due to tunable magnetic symmetry
Appl. Phys. Lett. **102**, 012403 (2013)

Enhancement of spin wave excitation by spin currents due to thermal gradient and spin pumping in yttrium iron garnet/Pt
Appl. Phys. Lett. **102**, 012401 (2013)

Charge density wave excitations in stripe-type charge ordered Pr_{0.5}Sr_{0.5}MnO₃ manganite
Appl. Phys. Lett. **101**, 252401 (2012)

Magnetostatic surface wave propagation in a one-dimensional magnonic crystal with broken translational symmetry
Appl. Phys. Lett. **101**, 242408 (2012)

Magnon scattering in single and bilayer graphene intercalates
J. Appl. Phys. **112**, 114308 (2012)

Additional information on *Appl. Phys. Lett.*

Journal Homepage: <http://apl.aip.org/>

Journal Information: http://apl.aip.org/about/about_the_journal

Top downloads: http://apl.aip.org/features/most_downloaded

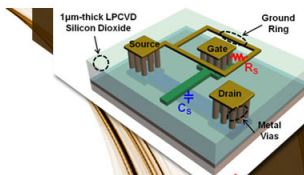
Information for Authors: <http://apl.aip.org/authors>

ADVERTISEMENT



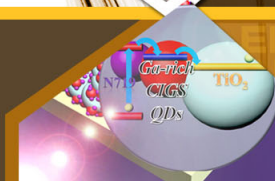
EXPLORE WHAT'S
NEW IN APL

SUBMIT YOUR PAPER NOW!



SURFACES AND INTERFACES

Focusing on physical, chemical, biological, structural, optical, magnetic and electrical properties of surfaces and interfaces, and more...



ENERGY CONVERSION AND STORAGE

Focusing on all aspects of static and dynamic energy conversion, energy storage, photovoltaics, solar fuels, batteries, capacitors, thermoelectrics, and more...

Excitation of propagating spin waves with global uniform microwave fields

Y. Au, T. Davison, E. Ahmad, P. S. Keatley, R. J. Hicken, and V. V. Kruglyak^{a)}
School of Physics, University of Exeter, Stocker Road, Exeter EX4 4QL, United Kingdom

(Received 13 December 2010; accepted 28 February 2011; published online 24 March 2011)

We demonstrate a magnonic architecture that converts global free-space uniform microwaves into spin waves propagating in a stripe magnonic waveguide. The architecture is based upon dispersion mismatch between the narrow magnonic waveguide and a wide “antenna” patch, both patterned from the same magnetic film. The spin waves injected into the waveguide travel to distances as large as several tens of micrometers. The antennas can be placed at multiple positions on a magnonic chip and used to excite mutually coherent multiple spin waves for magnonic logic operations. This demonstration paves way for “magnonics” to become a pervasive technology for information processing. © 2011 American Institute of Physics. [doi:10.1063/1.3571444]

At the current level of magnetodynamic experiments, even relatively small signal levels are sufficient to detect spin waves¹ propagating in magnonic waveguides. However, the prospects for magnonics and magnonic technology² depend on the availability of means for efficient injection of coherent spin waves into magnonic waveguides.³ The sought for well defined oscillatory phase relationship between *multiple* injection sites is not readily achievable by the methods of spin wave excitation demonstrated so far. Indeed, the most commonly used inductive excitation relies upon fabrication of impedance matched microantennas,⁴ which, however, suffer from increased Ohmic losses upon down scaling. Moreover, multiple current leads are required to deliver the microwave signal to antennas located at different positions on a “magnonic” chip, which will potentially present an architectural headache to circuit designers. The spin-transfer-torque (STT) based methods⁵ and those based on the vortex annihilation⁶ are broadband and truly nanoscale but unfortunately lack coherence. The phase locking between multiple STT oscillators was demonstrated in Ref. 7, but the compatibility of phase locking conditions with requirements of magnonic architectures has not been established. Ultrafast optical excitation⁸ is currently impractical for magnonic circuitry purpose due to the lack of compact (ideally, on-chip) sources of short optical pulses.

In this letter, we propose a wireless method of propagating spin wave excitation in which a uniform ferromagnetic resonance based antenna couples to free space microwaves (global and uniform from the antenna’s point of view) and converts them directly into finite wavelength spin waves propagating in stripe magnonic waveguides. The principle of action is based on dispersion mismatch at the boundary between the antenna and magnonic waveguide.⁹ The method is demonstrated here for micrometer scale devices using time resolved scanning Kerr microscopy (TRSKM).¹⁰ We discuss how this demonstration can pave way for future studies of nanoscale magnonic architectures.

Specifically, we studied a 110 nm thick Permalloy microstructure [Fig. 1(a)] formed on a 0.17 mm thick glass cover slip. The sample with Permalloy film facing up was overlaid onto a 0.5 mm wide central conductor of a coplanar waveguide made out of printed circuit board. The circuit was

used to deliver either pulses of 70 ps duration from a pulse generator or cw microwaves from a microwave generator to the sample. The pulse and microwave generators were synchronized with a Ti:sapphire laser producing ~ 100 fs optical probe pulses of 800 nm wavelength at the repetition rate of 80 MHz. The optical pulses were frequency doubled, and a microscope objective was used to focus them to a ~ 400 nm diameter circular spot on the sample surface. The pulsed or cw microwave magnetic field (h_{rf}) was modulated at a frequency of 3 kHz. The Kerr polarization rotation of the reflected optical pulse was then measured using an optical bridge detector and a lock-in amplifier. The detected signal was proportional to the out-of-plane component of the dynamic magnetization averaged over the optical spot area.

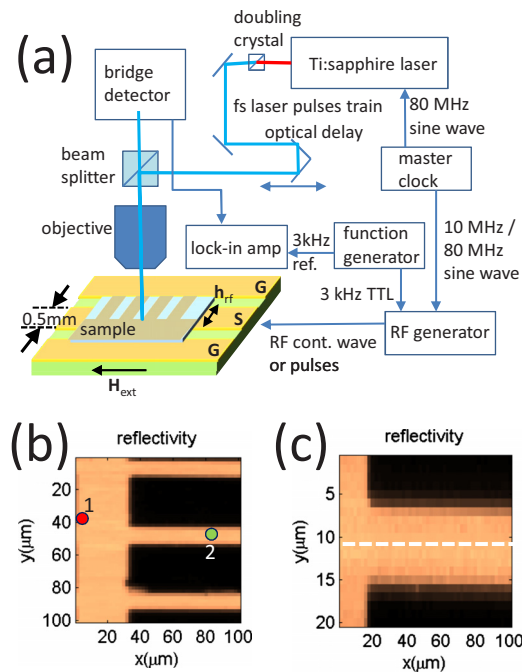


FIG. 1. (Color online) (a) The TRSKM experimental setup is schematically shown. The bias (H_{ext}) and dynamic magnetic field (h_{rf}) are perpendicular and parallel to the long axes of the stripes, respectively. (b) The scanned optical micrograph of the sample is shown, with bright representing the magnetic material. Dots 1 and 2 represent locations from which time resolved signals were acquired. (c) The enlarged portion of the image in (b) from which images of the dynamic magnetization were acquired is shown. The white dashed line indicates the line along which data shown in the right panel of Fig. 3 were acquired.

^{a)}Electronic mail: v.v.kruglyak@exeter.ac.uk.

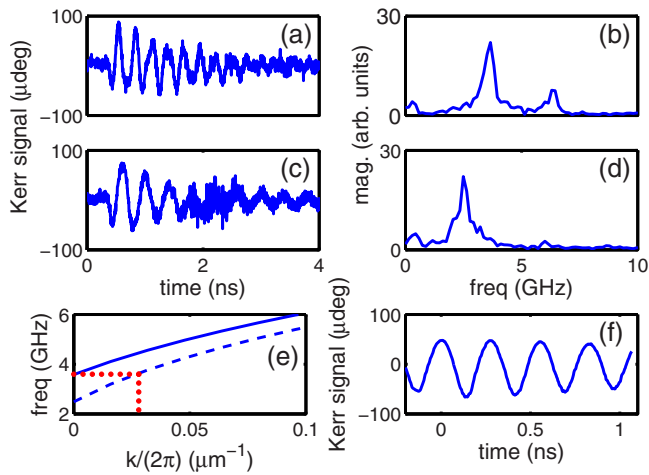


FIG. 2. (Color online) [(a) and (b)] The time resolved signal measured from dot 1 in Fig. 1(b) using pulsed excitation is shown together with its Fourier spectrum. [(c) and (d)] The time resolved signal measured from dot 2 in Fig. 1(b) using pulsed excitation is shown together with its Fourier spectrum. (e) The theoretical dispersions spin waves in the quasicontinuous film area (solid line) and in the stripe (dashed line) are shown. The dotted line indicates the hopping of the uniform precessional mode in the film into a finite wavelength mode in the stripe. (f) The time resolved signal in the continuous film region is shown for the excitation by a cw microwave at 3.60 GHz.

To acquire time resolved signals, a mechanical translation stage was used to vary the time of arrival of the optical pulses to the sample for a fixed position of the optical spot on the surface of the sample. To acquire images of the dynamic magnetization (i.e., Kerr rotation) at a fixed time of arrival of the probe pulse, a piezoelectric scanning stage was used to move the optical spot on the sample surface via scanning the objective lens within a horizontal plane parallel to the sample surface. The scanning also yielded a reflectivity image of the sample by simultaneously recording the dc intensity of light reflected from the sample.

Figure 1(b) presents a $100 \times 100 \mu\text{m}^2$ scanned reflectivity micrograph of the sample. The sample consists of millimeters long parallel microstripes of $10 \mu\text{m}$ width and $40 \mu\text{m}$ center to center spacing with one of their ends connected to a common millimeter-sized rectangular-shaped film region. The other ends of the stripes are beyond the present study.¹¹ The interstripe spacing is large enough to neglect any interaction between them. Figure 1(c) displays the part of the reflectivity image defining the boundary of the Kerr images shown later. As depicted in Fig. 1(a), the external in-plane static magnetic field (H_{ext}) and the dynamic magnetic field were perpendicular and parallel to the long axes of the stripes respectively.

First, we investigated the frequency response of the sample to a broadband excitation by the 70 ps magnetic pulses for a bias magnetic field of 154 Oe. Later we verified that the phenomenon of spin wave injection reported here was also observed at greater values of the applied field. First, the laser spot was placed at the point within the wide continuous film area, as indicated by a red dot (number 1) in Fig. 1(b). The measured time resolved signal and its Fourier spectrum are displayed in Figs. 2(a) and 2(b), respectively. The frequency of the dominant uniform precessional mode is 3.6 GHz, with a smaller peak also observed in the spectrum at 6.4 GHz. The results of similar measurements with the laser spot located at the point within the stripe indicated by the green dot (number 2) in Fig. 1(b) are shown in Figs. 2(c) and

2(d). The dominant uniform precessional mode has a frequency of 2.5 GHz, which is 1.1 GHz lower than in the continuous film part of the sample (red dot). This can be attributed to the reduction in the internal magnetic field in the stripe by the demagnetizing field due to the magnetic charges formed at and near the edges of the stripe.

The observed difference in the frequency of the uniform precessional modes in the stripe and continuous film constitute the basis of the proposed magnonic architecture. Indeed, the modes can be considered as magnetostatic spin waves with an infinite wavelength (i.e., with their wave vector $\mathbf{k} = 0$). Then, as plotted in Fig. 2(e), the dispersion of magnetostatic spin waves propagating inside the “continuous film” area and in the stripe in the direction perpendicular to the applied magnetic field (and hence parallel to the long axis of the stripe) will be different, with the relative frequency shift approximately equal to the difference between the frequencies of the two corresponding uniform modes. The plot suggests that the uniform precession of the continuous film ($\mathbf{k} = 0$ on the solid curve) should be able to leap into a spin wave mode with a finite \mathbf{k} value propagating inside the stripe as indicated by the red dotted line. The translational symmetry of the system is broken at the junction between the semi-infinite continuous film and the end of the stripe. This allows the uniform mode in the film to overcome the momentum gap, as required for the excitation of the nonuniform spin wave in the stripe. The latter spin wave is predicted to have a wavelength of about $36 \mu\text{m}$.

In order to verify the hypothesis, we excited the sample by a cw microwave with frequency of 3.60 GHz, which corresponds to the uniform mode inside the film, while keeping the external bias field unchanged at 154 Oe. The time resolved signal measured with the laser spot positioned inside the film area is plotted in Fig. 2(f). As expected, a harmonic signal was observed with the frequency equal to that of the exciting microwave field. Then, we acquired images of the dynamic magnetization in the area defined by the reflectivity image shown in Fig. 1(c) at different time delays at the time axis of Fig. 2(f). The results are shown in Fig. 3, left panel, (a)–(i). The particular values of time delay were chosen so as to span a single cycle of the magnetic precession [Fig. 2(f)].

First, we observe the film region to evolve from bright [Fig. 3, left panel, (a)] to dark [Fig. 3, left panel, (e)] and to bright [Fig. 3, left panel, (i)] again. This agrees with the fact that the film is driven in resonance with the excitation (pump) cw field. The color change in the film begins to occur near to the film edge [Fig. 3, left panel, (b) and (g)], indicating a phase lead of the precession at the film edge relative to the film interior. This is explained by the magnetization near the edge experiencing an effective field due to the magnetostatic charges dynamically formed at the edge. This boosts the effective magnetic field experienced by the edge magnetic moments. Therefore, the pump cw field is driving the moments below their natural resonance frequency, which gives rise to the observed phase lead.

Second, the entire stripe region becomes brighter at certain time delays [Fig. 3, left panel, (b), (c), and (d)] and darker for some other time delays [Fig. 3, left panel, (f), (g), and (h)]. This indicates that the precession inside the stripe lags behind that in the film, since the pump cw field is driving the wire above its resonance. This is consistent with the observed uniform resonance frequency of the stripe of 2.5 GHz [Fig. 2(d)], which is well below the pump frequency.

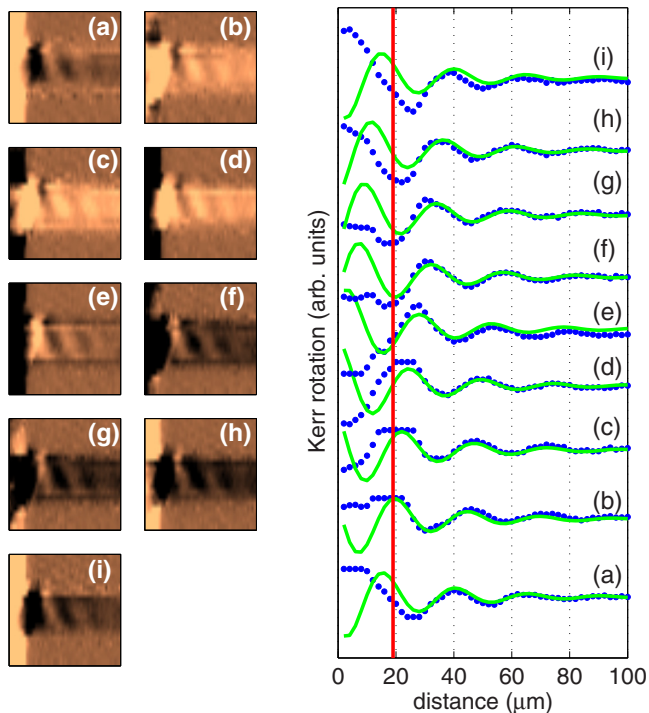


FIG. 3. (Color online) Left panel: images of the dynamic magnetization in the portion of the sample marked in Fig. 1(c) are shown for time delays of (a) 0.0 ps, (b) 46.7 ps, (c) 73.3 ps, (d) 100.0 ps, (e) 140.0 ps, (f) 186.7 ps, (g) 206.7 ps, (h) 233.3 ps, and (i) 273.3 ps, corresponding to the time axis of Fig. 2(f). Right panel: line scans along the white dashed line of Fig. 1(c) for images in the left panel are shown for the same set of time delays. The dots are experimental data and the curves are fits to a decaying harmonic wave form. The vertical line indicates position of the boundary between the stripe and film.

Third, which is most important in this study, we observe injection of spin wave ripples from the film into the stripe. The propagating nature of these ripples is more apparent when viewed through a computer animation.¹² The propagation of the ripples is also obvious from the line scan of the measured Kerr signal along the central axis of the stripe [white dashed line in Fig. 1(c)] in images shown in Fig. 3, as shown in the right panel of the same Figure with blue dots. The experimental data were fitted to a decaying harmonic wave form $\exp(-x/d) \cos(2\pi x/\lambda - 2\pi ft)$, where x is the distance along the stripe and t is time. For the excitation frequency $f=3.6$ GHz, the best fit to the data (blue dots) is obtained for wavelength λ and decay length d both equal to 25 μm , as shown by the green curves in the right panel of Fig. 3. The fitted wavelength is fairly comparable to the earlier predicted value of 36 μm .

In summary, we have demonstrated the injection of propagating spin waves into stripe magnonic waveguides by continuous film antennas. The latter act as magnonic sources—the key elements of envisaged magnonic chips.² The method does not require fabrication of narrow current leads to deliver the microwave signal to the excitation position but allows the excitation power to be drawn from free space microwaves. This ensures that the spin waves excited by multiple antennas are phase coherent as long as the size of the magnonic chip remains small compared to the microwave wavelength, typically of several millimeters. Information could be encrypted into the phase of the propagating spin waves emitted by different antennas, carried across the

chip along the stripes, and manipulated, as described in previous demonstrations either numerically¹³ or using mm scale devices.¹⁴ The basic concept of the uniform resonance frequency mismatch is not limited to devices formed from the same thin magnetic film.¹⁵ Our finding could make the magnonic information processing a feasible technology, while the method is expected to be useful in fundamental investigations in magnonics.

The authors gratefully acknowledge funding received from the EC's Seventh Framework Programme (FP7/2007-2013) under Grant Agreement No. 228673 (MAGNONICS) and from Engineering and Physical Sciences Research Council (EPSRC) of United Kingdom under Grant No. EP/E055087/1.

¹A. G. Gurevich and G. A. Melkov, *Magnetization Oscillations and Waves* (Chem. Rubber, New York, 1996).

²V. V. Kruglyak and R. J. Hicken, *J. Magn. Magn. Mater.* **306**, 191 (2006); V. V. Kruglyak, S. O. Demokritov, and D. Grundler, *J. Phys. D: Appl. Phys.* **43**, 264001 (2010); A. Khitun, M. Bao, and K. L. Wang, *ibid.* **43**, 264005 (2010).

³J. O. Vasseur, A. Akjouj, L. Dobrzynski, B. Djafari-Rouhani and E. H. Eloudouti, *Surf. Sci. Rep.* **54**, 1 (2004); R. Hertel, W. Wulfhekel, and J. Kirschner, *Phys. Rev. Lett.* **93**, 257202 (2004); S. V. Vasiliev, V. V. Kruglyak, M. L. Sokolovskii, and A. N. Kuchko, *J. Appl. Phys.* **101**, 113919 (2007); K.-S. Lee, D.-S. Han, and S.-K. Kim, *Phys. Rev. Lett.* **102**, 127202 (2009); K. Sekiguchi, K. Yamada, S. M. Seo, K. J. Lee, D. Chiba, K. Kobayashi, and T. Ono, *Appl. Phys. Lett.* **97**, 022508 (2010).

⁴S. Tamaru, J. A. Bain, R. J. M. van de Veerndonk, T. M. Crawford, M. Covington, and M. H. Kryder, *Phys. Rev. B* **70**, 104416 (2004); Z. Liu, F. Giesen, X. Zhu, R. D. Sydora, and M. R. Freeman, *Phys. Rev. Lett.* **98**, 087201 (2007); K. Perzlmaier, G. Woltersdorf, and C. H. Back, *Phys. Rev. B* **77**, 054425 (2008); V. Vlaminck and M. Bailleul, *Science* **322**, 410 (2008); V. E. Demidov, J. Jersch, S. O. Demokritov, K. Rott, P. Krzyszczo, and G. Reiss, *Phys. Rev. B* **79**, 054417 (2009); S. Neusser, G. Duerr, H. G. Bauer, S. Tacchi, M. Madami, G. Woltersdorf, G. Gubbiotti, C. H. Back, and D. Grundler, *Phys. Rev. Lett.* **105**, 067208 (2010).

⁵J. C. Sankey, P. M. Braganca, A. G. F. Garcia, I. N. Krivorotov, R. A. Buhman, and D. C. Ralph, *Phys. Rev. Lett.* **96**, 227601 (2006); M. R. Pufall, W. H. Rippard, S. E. Russek, S. Kaka, and J. A. Katine, *ibid.* **97**, 087206 (2006).

⁶S. Choi, K.-S. Lee, K. Y. Guslienko, and S.-K. Kim, *Phys. Rev. Lett.* **98**, 087205 (2007).

⁷S. Kaka, M. R. Pufall, W. H. Rippard, T. J. Silva, S. E. Russek, and J. A. Katine, *Nature (London)* **437**, 389 (2005); F. B. Mancoff, N. D. Rizzo, B. N. Engel and S. Tehrani, *ibid.* **437**, 393 (2005).

⁸M. van Kampen, I. L. Soroka, R. Brucas, B. Hjörvarsson, R. Wieser, K. D. Usadel, M. Hanson, O. Kazakova, J. Grabis, H. Zabel, C. Jozsa, and B. Koopmans, *J. Phys.: Condens. Matter* **17**, L27 (2005); B. Lenk, G. Eilers, J. Hamrle, and M. Münzenberg, *Phys. Rev. B* **82**, 134443 (2010); A. Kirilyuk, A. V. Kimel, and T. Rasing, *Rev. Mod. Phys.* **82**, 2731 (2010).

⁹V. E. Demidov, B. Hillebrands, S. O. Demokritov, M. Laufenberg, and P. P. Freitas, *J. Appl. Phys.* **97**, 10A717 (2005); V. E. Demidov, S. O. Demokritov, D. Birt, B. O'Gorman, M. Tsai, and X. Li, *Phys. Rev. B* **80**, 014429 (2009).

¹⁰M. R. Freeman and B. C. Choi, *Science* **294**, 1484 (2001); C. H. Back, D. Pescia, and M. Buess, *Top. Appl. Phys.* **101**, 137 (2006); V. V. Kruglyak, P. S. Keatley, A. Neudert, R. J. Hicken, J. R. Childress, and J. A. Katine, *Phys. Rev. Lett.* **104**, 027201 (2010).

¹¹See e.g., V. V. Kruglyak, P. S. Keatley, A. Neudert, M. Delchini, R. J. Hicken, J. R. Childress, and J. A. Katine, *Phys. Rev. B* **77**, 172407 (2008).

¹²See supplementary material at <http://dx.doi.org/10.1063/1.3571444> for movie.

¹³S.-K. Kim, *J. Phys. D: Appl. Phys.* **43**, 264004 (2010).

¹⁴A. B. Ustinov and B. A. Kalinikos, *Tech. Phys. Lett.* **29**, 602 (2003); T. Schneider, A. A. Serga, B. Leven, B. Hillebrands, R. L. Stamps, and M. P. Kostylev, *Appl. Phys. Lett.* **92**, 022505 (2008).

¹⁵Y. I. Gorobets, A. N. Kuchko, and S. V. Vasil'yev, *Fiz. Met. Metalloved.* **85**, 40 (1998).